A CASE RECORD OF DEEP EXCAVATION SUPPORTED BY STEEL PIPE SHEET PILES IN SEA RECLAMATION AREAS

Shuo Wang [1], Zurun Yue [2], Zhanhui Liu [3], and Yanjun Yang [4]

ABSTRACT

A group of deep excavations are operated in the sea reclamation area, Caofeidian, where the silt is thick, and the water is abundant because of the sea nearby. In this project, with the maximum excavation depth of 11.8 m, retaining structures of steel pipe sheet piles (SPSPs) with steel supports are applied, of which the longest piles are 24 m. Deformation laws of the excavation are presented by the observation of ground subsidence, displacements of pile tops, lateral movements of envelopes, axial forces of supports and varieties of groundwater level. The observational results are contrasted with the calculation results based on the equivalent beam method, and the influencing factors of the envelope deformation are analyzed by the same calculation method.

Key words: Sea reclamation area, steel pipe sheet piles, deep excavation, deformation.

1. INTRODUCTION

These excavation points are located in Caofeidian, China, where the silt is thick and the water is abundant. Because the filled sand is poor in the adhesion, it is difficult to dig and drill in this area. Steel pipe sheet piles (SPSPs) which are connected by large steel pipes and different kinds of joints, have been proved to avoid the difficulties of drilling successfully, and the construction efficiency is high. Furthermore, as temporary structures the SPSPs are convenient to remove, Gika and Toshinari introduce that SPSPs can replace the concrete pneumatic caisson as the cofferdam. Hereafter, transfer mechanism, impermeable performance and deformation mechanism, *etc* are studied in Japan (Risselada 1986; Abiko 1988; Fukuwaka 1997; Shimaoka 1998; Inazumi *et al.* 2005; Kimura *et al.* 2007). The SPSPs technology has been spread to many other countries and districts, such as China, Korea and Poland, *etc* (Kang 1991; Song 2007; Meng *et al.* 2002; Zhao *et al.* 2005).

2. PROJECT OVERVIEW AND GEOLOGICAL CONDITIONS

Excavation #18 and #19 in the groups are the research objects. They are retained by Φ1000 steel pipe piles which are connected by Φ200 steel pipes and H-beams as shown in Fig. 1. The thickness of Φ1000 and Φ200 steel pipes is 13 mm and 4 mm,

respectively. The excavation #18 is 11.8 m in depth, 30.2 m × 30.2 m in size, and the excavation #19 is 8.6 m in depth, 28.2 m × 14.5 m in size, as shown in Figs. 2 and 3.

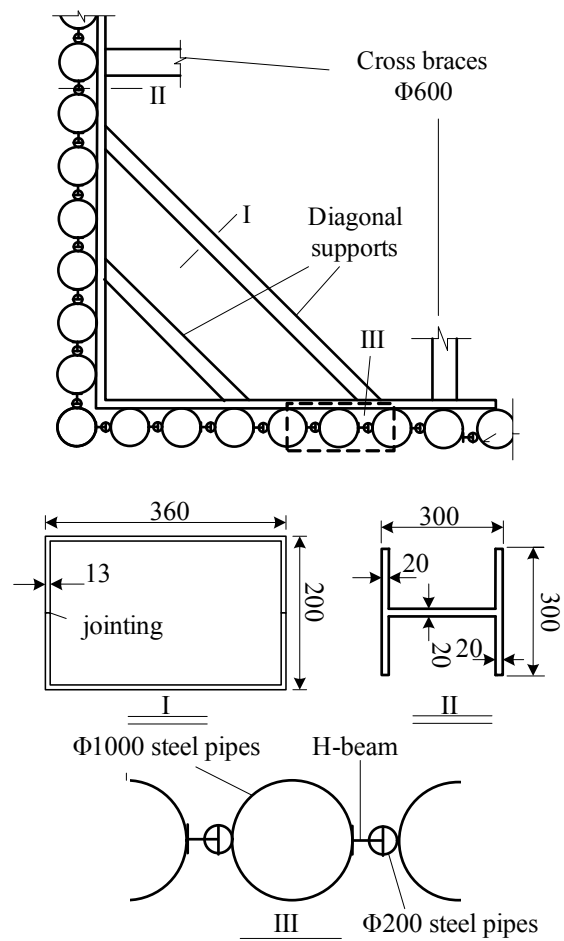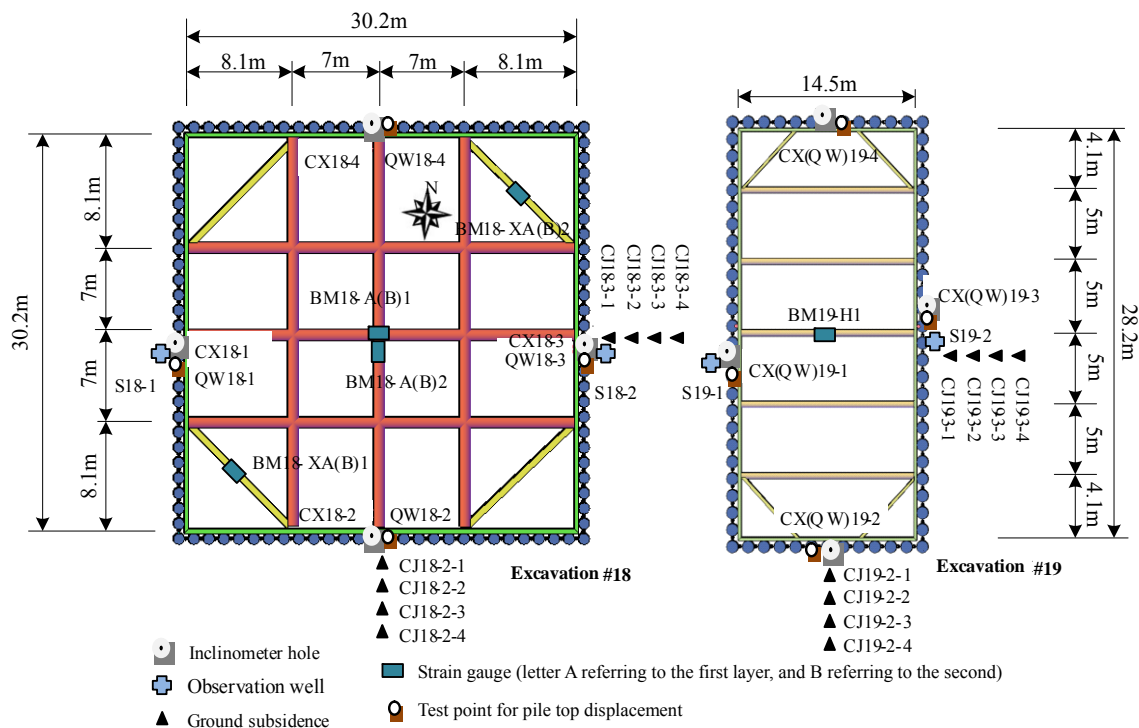**Fig. 1 Supporting system**

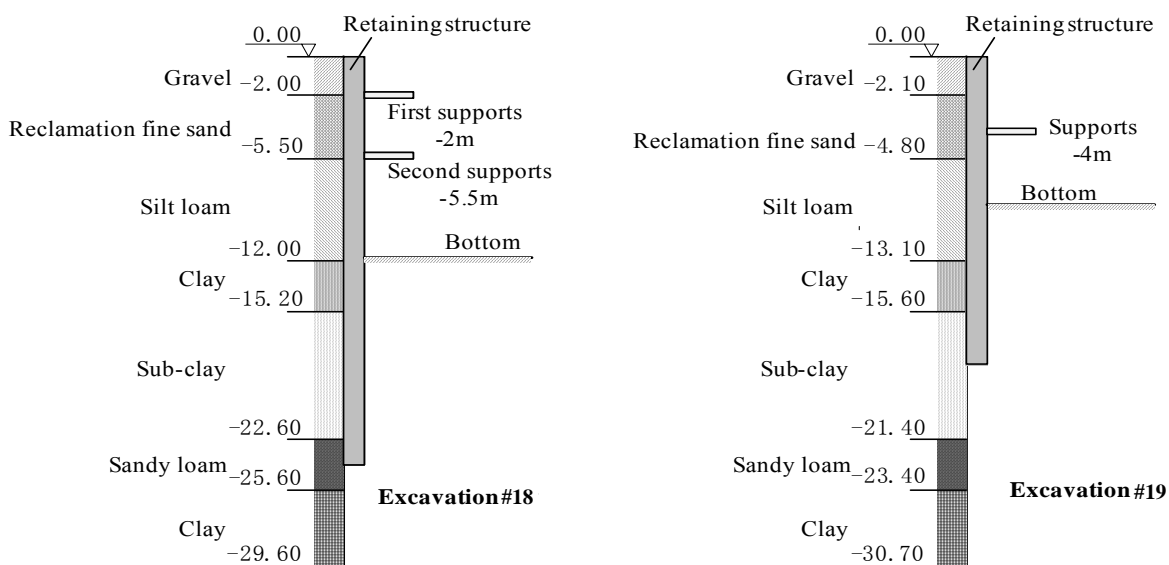**Fig. 2   Dimensions and gauge distribution in excavations**

Fig. 3   Vertical excavation profile and soil layers

The bottom of the retaining structures of the excavation #18 is at a depth of 24 m below the ground surface with the supports which are set at 2 m and 5.5 m below the ground surface respectively. The bottom of the retaining structures of the excavation #19 is at a depth of 18 m below the ground surface and the supports are set at 4 m below the ground surface, as described in Fig. 3. The cross braces are 600 mm in diameter, 13 mm in thickness. The diagonal supports are made by 2 【36a channel steel which is depicted in Fig. 1. In addition, Fig. 4 shows the supporting condition of the excavations in the field. The design loads of cross braces are 1400 kN and 1250 kN respectively in the excavation #18 and #19, and they are 1050 kN and 950 kN respectively for the

diagonal supports. The stiffness of the SPSPs, cross braces and diagonal supports are 525.4 kN-m², 112 kN-m² and 49.8 kN-m² respectively. The catchment and drainage pump are used as draining system, but the dewatering system is not installed.

The subsoil of the site is consisted of alternating clay and silty sand. The groundwater is of large amount due to the short replenishment route. As the groundwater level is between 3 to 3.5 m underground, the silty sand is totally saturated. As the pH value of groundwater is between 7.07 and 7.32, the underground steel and concrete structures will be corroded. Physico-mechanical parameters of soil layers are listed in Table 1.

(a) Excavation #18

(b) Excavation #19

Fig. 4   Supporting of excavations in field

Table 1   Physico-mechanical parameters of soil layers

Layer	Soil type	Thickness (m)	Unit weight (kN/m³)	c (kPa)	φ (°)	w (%)	w_p (%)	w_l (%)	SPT	S_u (kPa)
1	Gravel	1.8 ~ 2.5	20.1	0	36	–	–	–	15	–
2	Reclamation fine sand	2.2 ~ 4.7	20	5	21	30.5	19.3	32.5	6	–
3	Silt loam	4.8 ~ 8.2	19.2	14	12.3	30.2	18.6	30.0	–	5.2
4	Clay	2.7 ~ 3.8	18.2	17.3	10.7	36.2	24.0	46.0	–	26.8
5	Sub-clay	5.9 ~ 8.6	19.2	18.2	13.2	27.9	19.3	32.5	–	14.7
6	Sandy loam	2.2 ~ 6.7	19.1	13.6	15.5	19.3	17.4	28.7	–	22.7
7	Clay	3.2 ~ 5.1	18.7	32.1	13.2	28.4	22.7	31.6	–	41.3

3. MONITORING ITEMS AND MEASURING POINTS

Based on the geology, water condition and support scheme, monitoring items and instruments are listed in Table 2, and testing points are marked in Fig. 2. The distances of test points for ground subsidence are 2 m, 6 m, 15 m, 36 m in the excavation #18 respectively, and are 2 m, 6 m, 12 m, 24 m in the excavation #19 respectively.

4. OBSERVATION RESULTS

The excavation process is shown in Fig. 5.

Table 2   Monitoring items and instruments

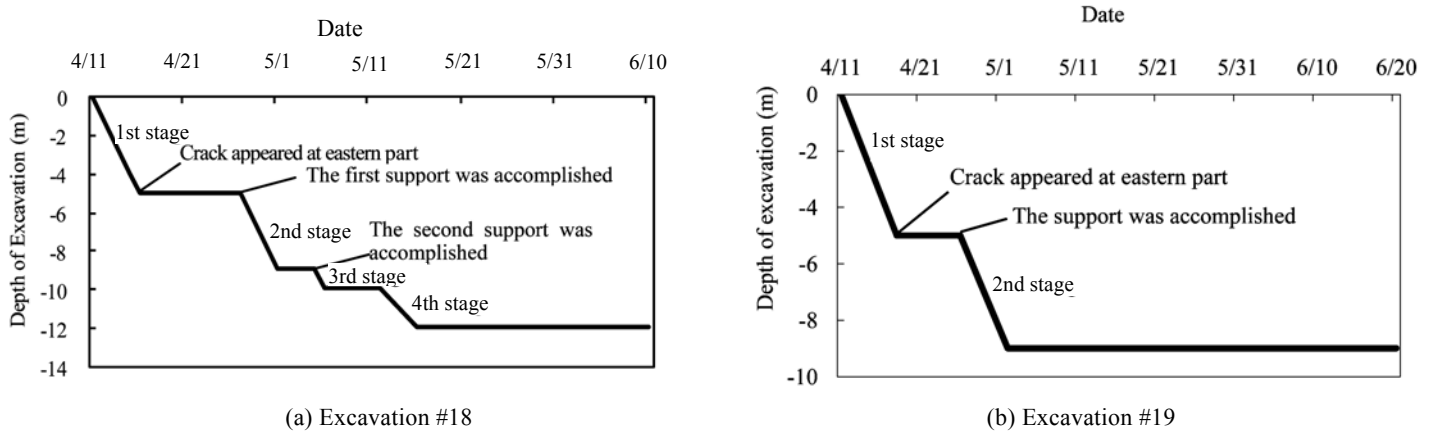| Monitoring items	Instruments
Lateral movements of envelopes	Inclinometer
Displacements of the pile tops	Total station, precision level
Ground subsidence	Precision level
Axial forces of supports	Strain gauge, frequency receiver
Groundwater level	Water level detector

(a) Excavation #18

(b) Excavation #19

Fig. 5   The process of excavation

4.1 Lateral Movements of Envelopes

Lateral Movements Along with the Depth

The lateral displacements of the measuring points are plotted in Figs. 6 and 7 respectively. The depths of inclinometer tip of CX18-2 and CX18-3 are 24 m and 20 m respectively; the depths of inclinometer tip of CX19-2 and CX18-3 are both 18 m. The inclinometer data have been revised based on displacement of pile top to obtain the actual movements of envelopes, because it is assumed no movement in the bottom of inclinometer.

Figures 6 and 7 demonstrate that:

(1) The horizontal displacements of piles are closely related to the process of excavation and support installation. A large amount of lateral movements are induced in the first and second stage of excavation. Subsequently, the pile tops appear to be stable and little movement restoration is observed till the end of excavation, which is evidenced by the small difference between the readings when excavation is at −8.5 m and at −11.8 m in Fig. 5, and when excavation is at −5 m and at −8.5 m in Fig. 6 (because the cracks appear behind CX18-3, the pile top movement is larger than the other three). The readings of CX18-3 indicate that the lateral wall movement decreases gradually in association of progress of the excavation. It is because the cracks behind CX18-3 are closed gradually after the supports are installed. The earth pressure behind CX18-3 is very little because of the cracks, but the earth pressure behind CX18-1 is still great, and the pressure is transferred to CX18-3 to force it move outward by the supports. All the movements of pile tops keep in large values, which are related to the mechanical properties of steel piles. Because the bending rigidity of steel pipe is worse than the concrete pile's, the support stiffness should be enhanced by installing the supports as early as possible and by increasing the intensity of the supports when the SPSPs are used.

(2) The position of maximum displacement is at 2 ~ 4 m above the bottom of excavation, the phenomenon is different with the observation result which is 2 ~ 4 m under the bottom of excavation in soft soil areas (Zhao *et al.* 2005).

(3) The maximum lateral movements which appear at −7.0 m, are −45.6 mm and −39.7 mm respectively in CX18-2 and CX18-3 when the deformation is stable. The lateral movements of different inclinometers are approximate at the same depth, though the stress paths are different.

(4) The maximum lateral movements are −37.3 mm and −51.8 mm respectively in CX19-2 and CX19-3 when the deformation is stable. So considering the maximum lateral movements in excavation #18, it is concluded that the pile deformation is influenced by the excavation size, and the pile deformation is greater as the excavation size becomes larger.

(5) Though the maximum lateral movements overstep the limitation in the codes (JGJ-99; GB 50497-2009), the support systems are steady in the total excavation process. Because the property of steel structure and concrete structure is different, and the existing codes for excavation design and construction are not formulated for SPSPs, the deformation mechanism of SPSPs should be studied in future, and the code for SPSPs design and construction should be prepared.

Lateral Movements Along with the Time

The readings obtained at different depths are shown in Fig. 8. Two conclusions are analyzed by Fig. 8:

(1) The pile deformations increase gradually along with the development of excavation in different depths. The locations of the maximum deformation move down gradually along with the procedure of excavation and support installation.

(2) The growth rates decrease from the pile top to the pile bottom gradually before the supports are installed. The movements increase much more at the level "−8 m" and "−14 m" for about 10 days after the excavation is finished. However, the movements of each level in CX19-3 develop greatly in the two stages, and the trends are not influenced by the supports. The movements are opportunely stable after the excavation is accomplished in CX19-3. The time effect isn't observed clearly when the non-supported depth is 50% more than the total depth in the single support system.
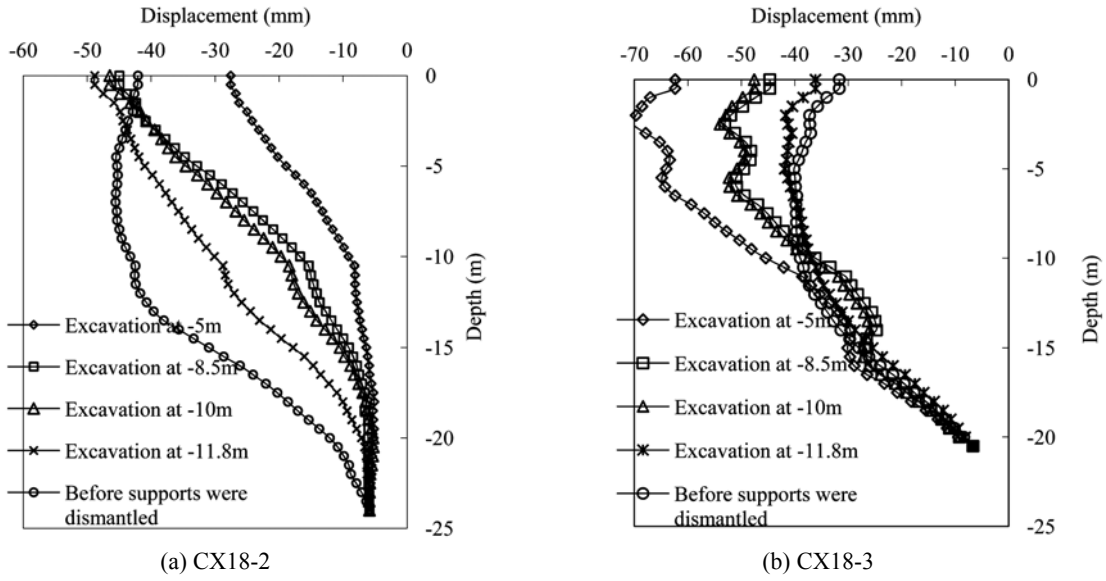
(a) CX18-2   (b) CX18-3

Fig. 6   Relationship curves of horizontal displacement vs. depth in excavation #18

(a) CX19-2   (b) CX19-3
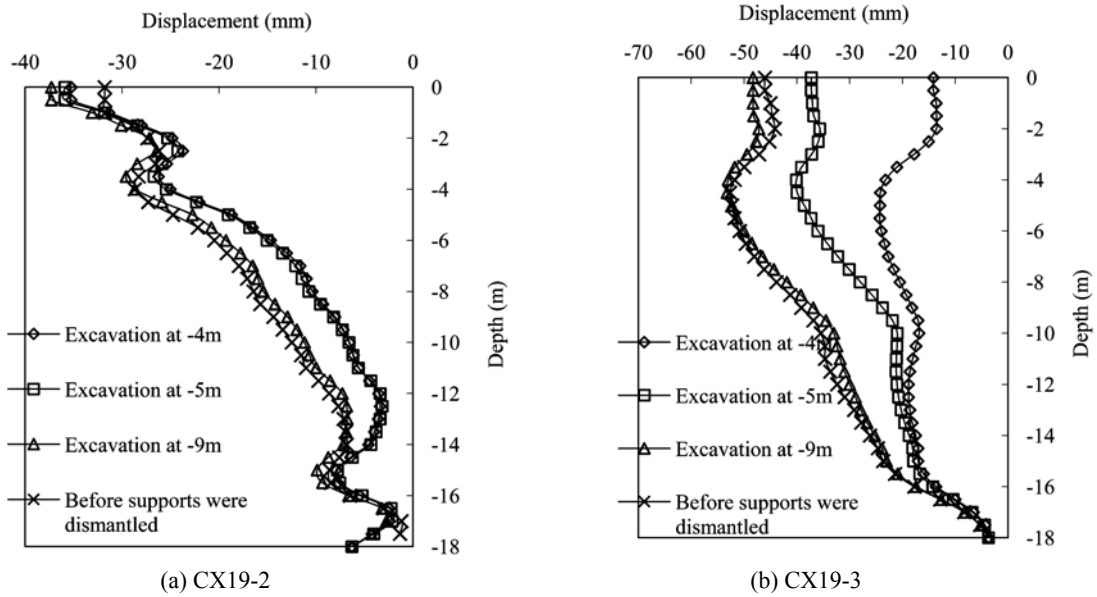
Fig. 7   Relationship curves of horizontal displacement vs. depth in excavation #19

(a) CX18-2   (b) CX19-3
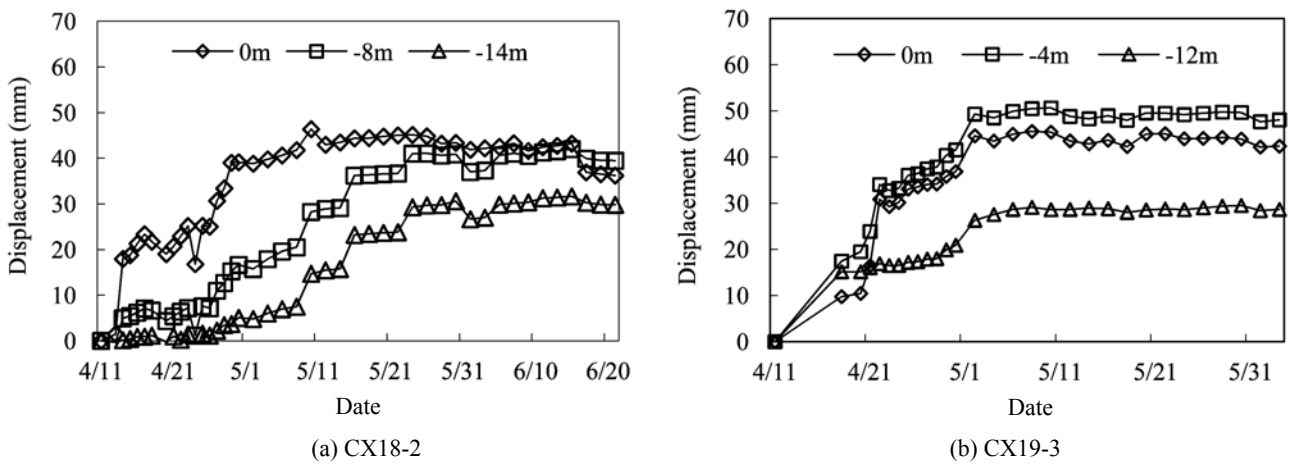
Fig. 8   Lateral movements of inclinometer CX19-3 at different depths

4.2 Displacements of the Pile Tops

Horizontal and vertical displacements of the pipe tops are measured respectively. The subsidence and uplift of pile top are plotted in Fig. 9. The vertical movements of pile top are surveyed by the precision level. Measuring points are installed by melting the steel bars, 5 cm in length and 1 cm in diameter, on the top of the steel pipes; 3 base points which are more than 50 m away from the excavations, are installed by drilling hole, 5 m in length and 10 cm in diameter, and cementing the steel bars. The steel bars which are protected by steel covers, are exposed 10 cm above the ground.

As plotted in Fig. 9, the direction of vertical displacements of pipe tops is upward until about 50% of the excavation has been finished after a little decline. It is very different from other trends which appear in the other envelopes such as diaphragm walls, bored piles and mixing piles. When steel pipe piles are driven into soil, they are compressed by frictional resistance, however, the amount of compression is released after the soil is excavated, consequently the uplift occurs. The pile tops go down continuously about 25 days after the excavation is accomplished. The maximum subsidence is 20.11 mm and 21.03 mm respectively in the excavation #18, and it is 10.45 mm and 12.57 mm respectively in the excavation #19. The subsidence of the excavation #18 is more than it of the excavation #19, so the vertical displacements are influenced by the excavation depth, and the maximum subsidence is about 0.15% of the excavation depth.

4.3 Groundwater Level

The gullies are dug in the excavation and the pooling of water is pumped by the draining system, but the dewatering well is not sited. As shown in Fig. 10, most variations of groundwater appear in the process of excavation. After the completion of excavation, little changes are observed. Because the water level decreases steadily, it is concluded that the sealing effect of the SPSPs is well, and it doesn't need to construct waterproof curtain.

4.4 Ground Subsidence

Figure 11 plots the ground subsidence along with the excavation process which is shown in Fig. 5. As it is noted from the readings, the most subsidence is induced during the excavating phase. The subsidence appears stable and little settlement is observed after the end of excavation. The results are supported by the readings obtained on 17 May to 10 June in the excavation #18 and those obtained on 2 May to 10 June in the excavation #19. The subsidence of the excavation #18 is much more than it of the excavation #19, so it is obvious that the ground subsidence increases along with the excavation depth. In addition, the time curve of ground subsidence and groundwater variation is accordant. It is also noticed that the subsidence of the locations, which are 3 times of the excavation depth behind the envelopes is kept in large value.
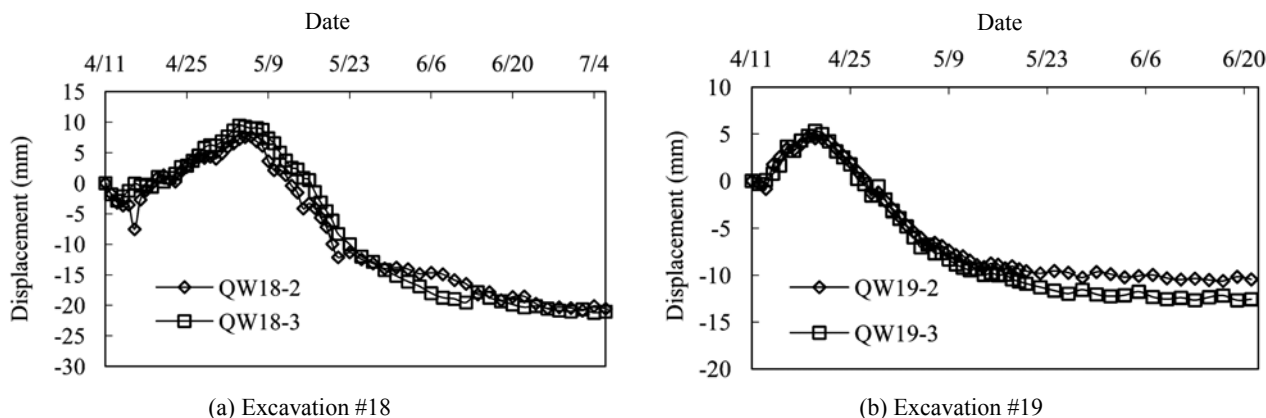

(a) Excavation #18

(b) Excavation #19
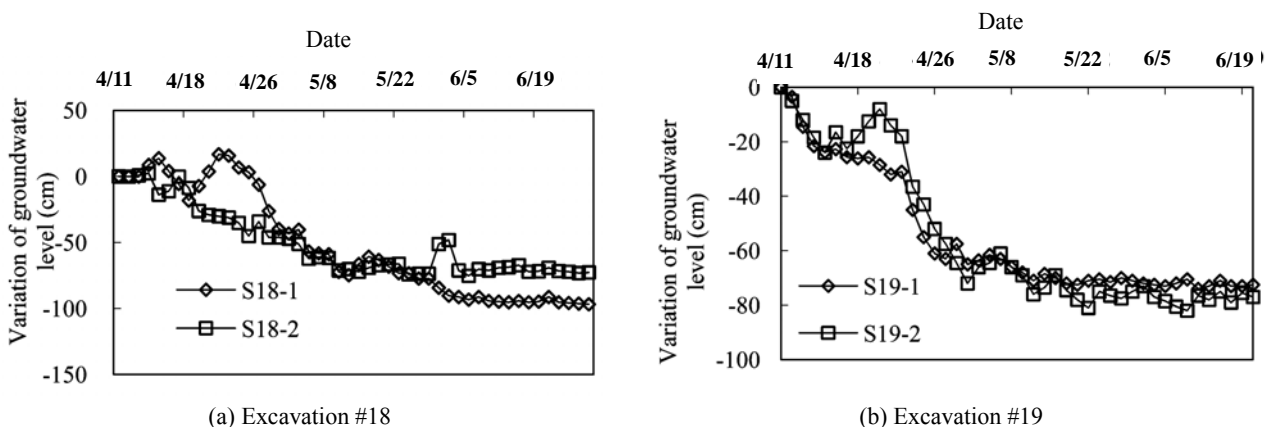
Fig. 9   Vertical displacements of pile tops

(a) Excavation #18

(b) Excavation #19

Fig. 10   Variations of groundwater level at various time
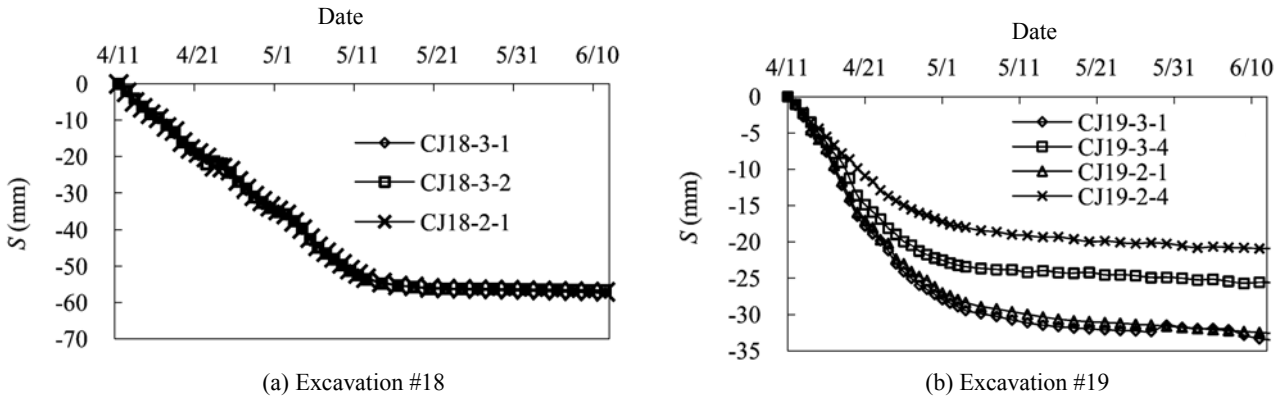
(a) Excavation #18

(b) Excavation #19

Fig. 11   Ground subsidence along with time

Figure 12 displays the subsidence of points CJ18-2-1 ~ CJ18-2-4 at different time. It is noticed that the subsidence reduces heavily at CJ18-2-4 which is 3 times of the excavation depth away from the excavation, though the subsidence remains in a large value.

4.5 Axial Forces of Supports

Axial Forces of Cross Braces

The axial forces of cross braces along with the time are plotted in Fig. 13, and the minus means the supports suffer pressure.

The most axial forces appear in the process of excavation. Because the supports are installed when the excavations are at −5 m, the axial forces of cross braces are less than the 20% of the design values. Accordingly, the design of supports should be optimized by taking the installation time of the supports into account. The axial forces of cross braces appear stable or present a little variation about 10 days after the accomplishment of excavation. The forces of second supports are larger than those of first supports in the excavation #18, and the phenomenon is accordant with the deformation of envelopes.

Axial Forces of Diagonal Braces

It is noticed in Fig. 14 that the axial forces of diagonal braces not only are larger than those of cross braces, but also become stable faster. Because the diagonal braces are installed earlier and the stress condition is more complicated, the readings of the forces of diagonal braces are much more than them of cross supports. Based on the results, the design forces of supports in this case are not suitable, and the design forces of diagonal braces should be more than the design forces of cross supports actually. It is also noted that the installation of diagonal braces is very useful for deformation control of the excavations in the sea reclamation areas, and they should be installed earlier than cross braces.

As depicted in Fig. 15, BM18-X11 is set on the top surface, BM18-X12 is set on the bottom surface, BM18-X13 is set on the side which is adjacent to the envelop piles, BM18-X14 is set on the other side. The stresses of four testing points in BM18-XA1 are plotted in Fig. 16. It is noticed that the trends of stresses are complicated in the excavation process, but the stresses of the points BM18-X11 and BM18-X14 are greater than the opposite points' results. Figure 17 presents the stresses of diagonal braces.
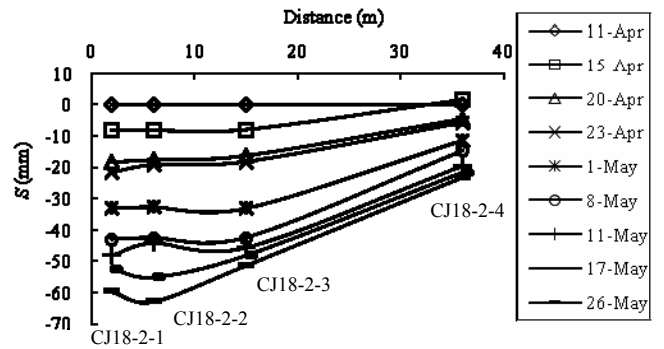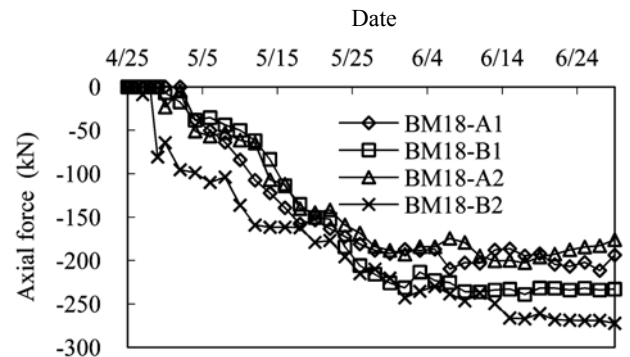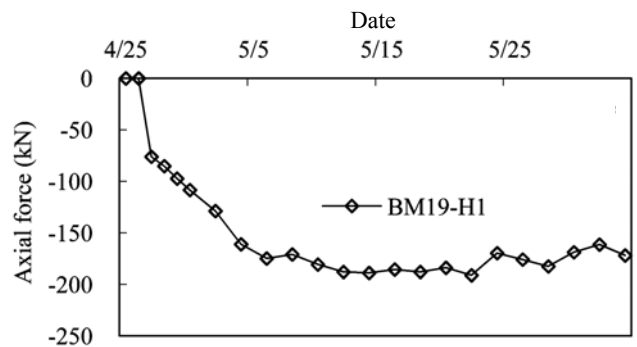

Fig. 12   Ground subsidence along with distance

(a) Excavation #18

(b) Excavation #19

Fig. 13   Axial forces of cross braces

5. COMPARISON OF CALCULATION WITH TESTING RESULTS

Equivalent beam method is used to calculate the deformation of the excavation #18 based on the principle of equal rigidity. Fig. 18 indicates the deformation in different phases, and the last ground surface settlement which is calculated by the Tongji parabola method, is presented in Fig. 19. Parameters for calculation are listed in Table 1.

By the comparison of calculation with testing results, it is concluded that:

1. The maximum calculation deformation is about 31.4% more than the testing results at most (taking out the influence of cracking) when the excavation is accomplished.

2. Based on the calculation, the transformative form of the enclosure structures is similar to the testing results in the excavation process. It is noted that the deformation of the pile top is large in all the steps, however, the calculation results cannot reflect the withdrawal of deformation in pile tops after the excavation has been finished.

3. The maximum settlement (48 mm) of the ground surface behind the envelopes is less than the observation result, furthermore, the range of observational settlements is larger, so the parabola method cannot calculate the subsidence of surface in the sea reclamation areas.

6. INFLUENCE FACTORS FOR DEFORMATION

The impact of each factor is calculated by a software which is based on the equivalent beam method.

6.1 Non-Supported Depth

As indicated in Fig. 20, the maximum displacement of the pile top grows exponentially as the non-supported depth increases. Equation (1) is presented to calculate the maximum displacement of pile top in the sea reclamation areas.

$$s = 1.348 \, e^{0.693h} \tag{1}$$

where h is non-supported depth, m; s is the maximum displacement in pile top, mm.

6.2 Bending Stiffness of Envelopes

As shown in Fig. 21, the increase of bending stiffness of envelopes can prevent deformation effectively until the sectional moment of inertia comes into 1,000,000 cm⁴. The movements of "Top" and "Bottom" appear stable when the sectional moment of inertia is larger than 1,000,000 cm⁴, so it is meaningless to enlarge the bending stiffness too much. In addition, the passive earth pressure will increase if the bending stiffness is too much.
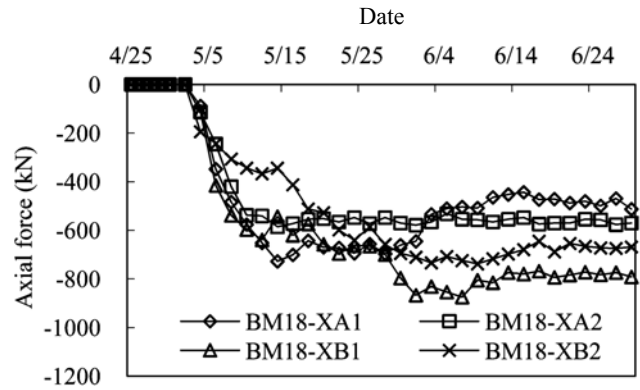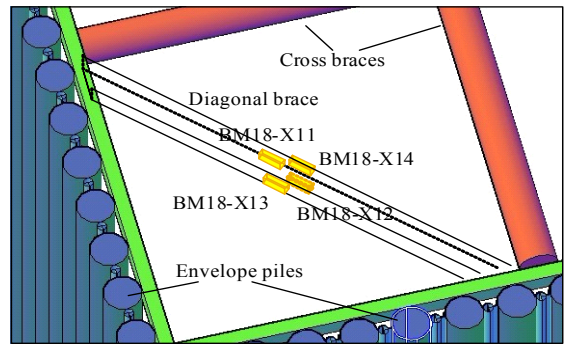

Fig. 14   Axial forces of diagonal braces

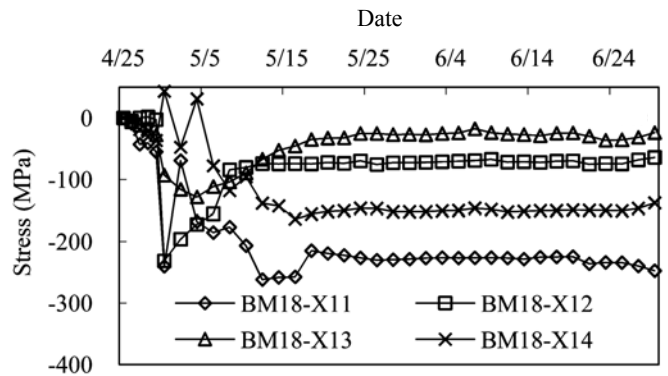**Fig. 15   Gauges distribution in diagonal brace**

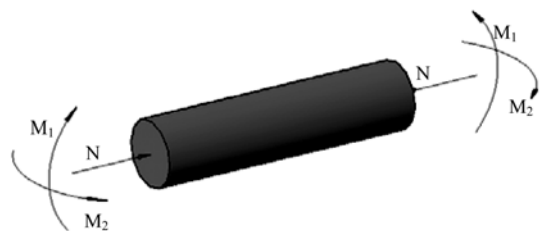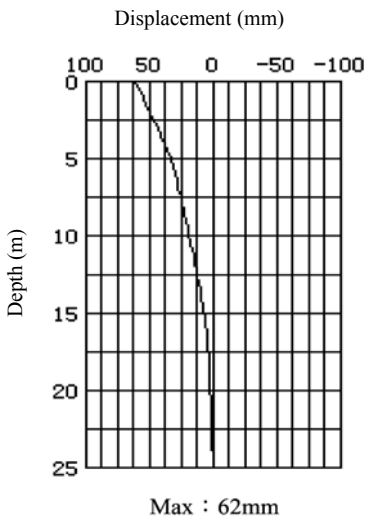**Fig. 16   The stresses of different position in BM18-XA1**
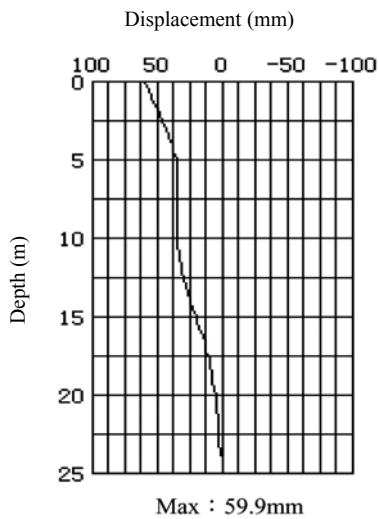

Fig. 17   The force model of diagonal brace

Displacement (mm)
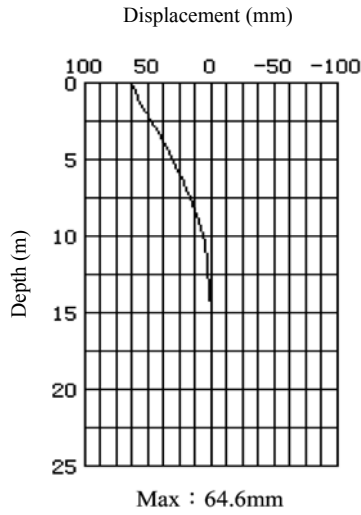
(a) Excavation at −5 m

Displacement (mm)

(b) Excavation at −8.5 m supports are finished

Displacement (mm)

(c) Excavation at −11.8 m supports are finished

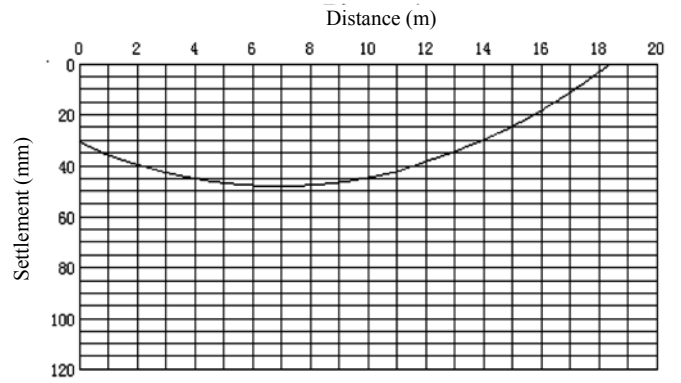**Fig. 18 Calculation deformation of excavation #18**

Distance (m)

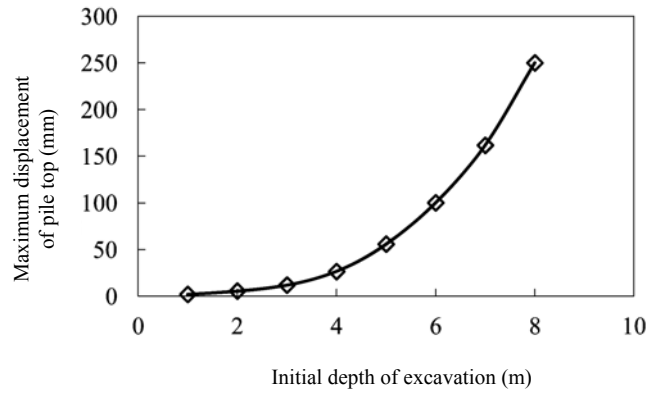**Fig. 19 Final settlement of ground surface**

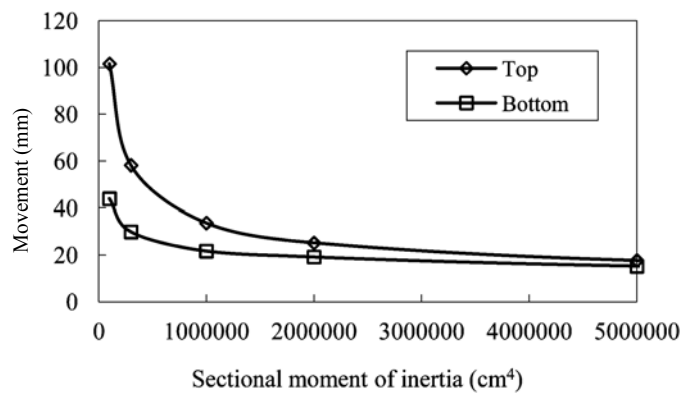**Fig. 20 Relationship between non-supported depth and maximum displacement of pile top**

Fig. 21 Relationship between sectional moment of inertia and the maximum movement of pile at top/bottom

7. CONCLUSIONS

The foregoing discussions lead to the following conclusions:

1. The pile tops move largely if no-support excavation is excessive. The maximum deformations of envelope piles are in the range of 2 ~ 4 m above the bottom, and the deformations of enclosure piles present "parabola" mode.

2. The envelope piles uplift until 50% of the excavation is finished. The maximum subsidence of the enclosure pile is 0.15% of the excavation depth.

3. The waterproof effect of SPSPs is proved well in the sea reclamation areas.

4. The amount of ground subsidence increases along with the excavation depth. More than 80% of the total subsidence achieves in the excavating period. In addition, the subsidence reduces heavily at the point which is 3 times of the excavation depth away from the envelopes, though it remains in a large value.

5. If the excavation is supported by two layers of bracings, the axial forces of the first layer supports can be stable in 5 days after the completion of excavation, however, the axial forces of the second layers are stable in 15 days. Moreover, the axial forces in diagonal braces are 2 to 4 times of the forces in cross braces.

6. The optimum non-supported depth is 2 m. The bending stiffness of envelopes can prevent deformation effectively until the sectional moment of inertia comes into 1,000,000 cm^4.

REFERENCES

Abiko, T., Kujirai, H., Izumi, and K., Morimoto, A. (1988). "Studies on the joint structure between footing concrete and steel sheet pipe pile wall." *Proceedings of the Japan Society of Civil Engineers*, **8**(390), 47–56 (in Japanese).

Chinese Academy of Building Research (1999). "JGJ-99 technical specification for retaining and protection building foundation excavation." *China Architecture and Building Press*, Beijing, China (in Chinese).

Construction Department of Shandong Province (2009). "GB 50497-2009 technical code for monitoring of building excavation engineering." *China Architecture and Building Press*, Beijing, China (in Chinese).

Fukuwaka, M., Shinomiya, H., and Furuya, H. (1997). "Large scale maritime structures using steel pipe piles." *Kawasaki Steel Technical Report*, **36**, 41–47.

Inazumi, S., Kimura, M., Yamamura, K., Nishiyama, Y., and Kamon, M. (2005). "Construction of vertical cutoff barrier using H-jointed steel pipe sheet piles with H-H joints." *Journal of the Society of Materials Science*, **54**(11), 1105–1110 (in Japanese).

Kang, B. H. (1991). "Static bearing capacity of an open-ended steel pipe pile driven into sand deposit." *Journal of Korean Geotechnical Society*, **26**(7), 111–116 (in Korean).

Kimura, M., Inazumi, S., Too, J., Isobe, K., Mitsuda, Y., and Nishiyama, Y. (2007). "Development and application of H-joint steel pipe sheet piles in construction of foundations for structures." *Soils and Foundations*, **47**(2), 237–251.

Meng, G. and Liu X. (2002). "Design and construction for sealed steel tube purdah stake in major thrustful foundation." *Bridge Construction*, **32**(5), 67–70 (in Chinese).

Risselada, T. (1986). "Application of tubular steel pipes as structural elements for retaining walls." *Dock and Harbor Authority*, **66**(776), 215–220.

Shimaoka, H., Nakagawa, S., Husamae, M., Nagayama, H., Shintani, T., and Onda, K. (1998). "Steel sheet pile with drain pipe 'Drain SP'." *NKK Technical Review*, **79**, 46–53.

Song, Y. (2007). "Application of interlocking steel tube piles cofferdam." *Western China Communications Science & Technology*, **2**(3), 71–74. (in Chinese).

Zhao X., Li B., and Yang G. (2005). "Practice and theory of large ultra-deep foundation." *China Communications Press*, Beijing, China (in Chinese).